Historical Biology

An International Journal of Paleobiology

ISSN: 0891-2963 (Print) 1029-2381 (Online) Journal homepage: http://www.tandfonline.com/loi/ghbi20

A fourth mandible and associated dental remains of Gigantopithecus blacki from the Early Pleistocene Yanliang Cave, Fusui, Guangxi, South China

Yingqi Zhang, Changzhu Jin, Reiko T. Kono, Terry Harrison & Wei Wang

To cite this article: Yingqi Zhang, Changzhu Jin, Reiko T. Kono, Terry Harrison & Wei Wang (2016) A fourth mandible and associated dental remains of Gigantopithecus blacki from the Early Pleistocene Yanliang Cave, Fusui, Guangxi, South China, Historical Biology, 28:1-2, 95-104, DOI: 10.1080/08912963.2015.1024115

To link to this article: http://dx.doi.org/10.1080/08912963.2015.1024115

Historical Biology, 2016
Vol. 28, Nos. 1–2, 95–104, http://dx.doi.org/10.1080/08912963.2015.1024115

A fourth mandible and associated dental remains of *Gigantopithecus blacki* from the Early Pleistocene Yanliang Cave, Fusui, Guangxi, South China

Yingqi Zhang[a]*, Changzhu Jin[a], Reiko T. Kono[b], Terry Harrison[c] and Wei Wang[d]

[a]*Key Laboratory of Vertebrate Evolution and Human Origins, Institute of Vertebrate Paleontology and Paleoanthropology (IVPP), Chinese Academy of Sciences, P.O. Box 643, Beijing 100044, P.R. China;* [b]*Department of Anthropology, National Museum of Nature and Science, Tsukuba 305-0005, Japan;* [c]*Department of Anthropology, Center for the Study of Human Origins, New York University, New York, NY 10003, USA;* [d]*Guangxi Museum of Nationalities, Nanning 530021, P.R. China*

(*Received 13 December 2014; accepted 25 February 2015*)

Dentognathic remains of *Gigantopithecus blacki* from the newly discovered Early Pleistocene locality of Yanliang Cave, Guangxi, South China are described. These include an incomplete mandible, only the fourth discovered and the first known from a site other than Liucheng, as well as 25 isolated teeth. Comparisons of the Yanliang mandible show that the best preserved part of the right corpus is morphologically similar to the left side of the Liucheng Mandible III. In addition, the Yanliang mandible and the Liucheng Mandible III share a similar degree and pattern of wear on the premolars and molars. The partially resorbed alveolus for the right M_2 in the Yanliang mandible indicates antemortem tooth loss, which is the first record of its kind for *Gigantopithecus blacki*. Comparisons of the enamel–dentine junction morphology show that the isolated upper premolars from Yanliang are similar to those of *Gigantopithecus* blacki from Early Pleistocene sites, and differ from the more specialised form from the Middle Pleistocene Hejiang Cave. This supports the biochronological evidence that Yanliang Cave is Early Pleistocene in age.

Keywords: *Gigantopithecus blacki*; hominoid; Pleistocene; antemortem tooth loss; enamel–dentine junction

Introduction

The extinct giant ape *Gigantopithecus blacki* was initially named by von Koenigswald (1935) based on an isolated right M_3 obtained from a Hong Kong drugstore, where it was being sold for traditional Chinese medicine. Over two decades later, three teeth of *Gigantopithecus blacki* were discovered *in situ* in Hei Cave, Daxin County, Guangxi (Pei and Woo 1956). These finds shed important light on the provenance and geological age of *Gigantopithecus*. Later that same year, two partial mandibles of *Gigantopithecus blacki* were discovered *in situ*, with the help of a local farmer, in the *Gigantopithecus* Cave (Xiaoyan Cave) of Liucheng County, Guangxi nearly 300 km NE of Hei Cave (Pei 1957). The following field seasons at the site yielded a third mandible (Pei and Li 1958) and over 1000 isolated teeth (Woo 1962). During the 1970s, several other *Gigantopithecus*-bearing localities were reported (Chang et al. 1973, 1975; Hsu et al. 1974), but the collections were limited to isolated teeth. This first wave of discoveries, primarily by researchers from the Institute of Vertebrate Paleontology and Paleoanthropology (IVPP), resulted in a much improved understanding of the phylogenetic relationships and palaeobiology of *Gigantopithecus* (e.g. Weidenreich 1945; von Koenigswald 1952, 1958; Woo 1962; Eckhardt 1975; White 1975; Szalay and Delson 1979; Zhang 1982; Ciochon et al. 1990; Daegling and Grine 1994; Han and Zhao 2002; Kelley 2002; Cameron 2003; Zhao and Zhang 2013). However, the lack of cranial and postcranial material of *Gigantopithecus blacki*, due to preservational and taphonomic factors (White 1975), has seriously hampered a more comprehensive understanding of the species. More recent excavations at cave sites in Guangxi by researchers of the IVPP and the Natural History Museum of Guangxi (NMHG) (Wang et al. 2005; Wang 2009; Jin et al. 2009; Takai et al. 2014; Zhang, Jin, et al. 2014; Zhang, Kono, et al. 2014) have also yielded collections that consist entirely of dental remains. Over the past decade, our team, led by Changzhu Jin, has systematically investigated caves in the Chongzuo area in Guangxi, and has excavated more than 10 Pleistocene sites with abundant fossil remains (Jin et al. 2009; Takai et al. 2014; Zhang, Jin, et al. 2014; Zhang, Kono, et al. 2014). Eight of these sites have yielded the remains of *Gigantopithecus blacki*. The newly discovered remains are all isolated teeth except for an incomplete mandible of *Gigantopithecus blacki* from Yanliang Cave discovered in 2011. This is only the fourth partial mandible of *Gigantopithecus blacki* recovered, and the only one known from a site beyond Liucheng. In view of its importance, the Yanliang mandible is described in the present paper, along with the isolated teeth from the site. We dedicate this paper to Dr. Yukimitsu Tomida, an old

*Corresponding author. Email: zhangyingqi@ivpp.ac.cn

Table 1. Specimen list and measurements (mm) of *Gigantopithecus blacki* from Yanliang Cave, Fusui, Guangxi.

IVPP no.	Field no.	Identification	MD	MAXOB	MDMAX	BL	PP
PA1601-1	CFLGYL201111-800	Right P_3		22.1			15.7
		Right M_1	20.1			17.9	
		Right M_3	21.6			17.3	
PA1601-2	CFLGYL201111-801	Left M_2	20.6			19.7	
		Left M_3	20.3			17.8	
PA1602.1	CFLGYL201111-812	Left I^1	15.0			15.1	
PA1602.2	FLGY201104-GY-1-7	Right C^1		16.1			15.9
PA1602.3	FLGY201104-GY-1-33	Right C^1		17.0			15.8
PA1602.4	CFLGYL201111-808	Left P^3			14.8	20.9	
PA1602.5	CFLGYL201111-809	Left P^3			13.7	20.3	
PA1602.6	CFLGYL201111-810	Right P^3			17.1		
PA1602.7	CFLGYL201111-803	Left $M^{1/2}$					
PA1602.8	CFLGYL201111-802	Left M^3	20.5			22.1	
PA1602.9	CFLGYL201111-815	Left I_1				9.7	
PA1602.10	FLGY201104-GY-1-26	Left I_2	8.4			11.1	
PA1602.11	FLGY201104-GY-1-36	Left I_1	7.8			10.6	
PA1602.12	FLGY201104-GY-1-336	Left I_1	7.2			9.5	
PA1602.13	FLGY201104-GY-1-6	Left P_3		20.9			15.4
PA1602.14	FLGY201104-GY-1-322	Left P_3		19.2			15.3
PA1602.15	CFLGYL201111-811	Right P_3					
PA1602.16	FLGY201104-GY-1-2	Left P_4	14.8			17.0	
PA1602.17	FLGY201104-GY-1-323	Left P_4	17.0			18.6	
PA1602.18	CFLGYL201111-804	Right M_1	19.2			17.3	
PA1602.19	FLGY201104-GY-1-3	Left M_1	18.9			16.8	
PA1602.20	FLGY201104-GY-1-5	Left M_1	17.8			17.3	
PA1602.21	CFLGYL201111-805	Right M_2	21.1			18.4	
PA1602.22	FLGY201104-GY-1-1	Left M_3	25.3			21.4	

friend and mentor to the lead author, on the occasion of his retirement next year from National Museum of Nature and Science (NMNS).

Materials and methods

Institutional abbreviations

IVPP, Institute of Vertebrate Paleontology and Paleoanthropology, Chinese Academy of Sciences, Beijing, China; PA, palaeoanthropological collection numbers of IVPP; KLVEHO, Key Laboratory of Vertebrate Evolution and Human Origins, Chinese Academy of Sciences, Beijing, China; IHEP, Institute of High Energy Physics, Chinese Academy of Sciences, Beijing, China; NHMG, Natural History Museum of Guangxi, Nanning, Guangxi, China; NMNS, National Museum of Nature and Science, Tokyo, Japan.

Location, age and geological context of the material

The *Gigantopithecus blacki* specimens (Table 1) described here were obtained from Yanliang Cave (22°13′54″N, 107°36′35″E), Fusui County, Chongzuo City, Guangxi, during the spring and autumn field seasons in 2011. Yan et al. (2014) and Zhu et al. (2014) list at least 40 mammalian taxa associated with *Gigantopithecus blacki*, and consider the age of the fauna to be Early Pleistocene based mainly on biostratigraphic correlations and the relative elevation of the cave systems (Yan et al. 2014; Zhu et al. 2014).

Measurements and methods

The molar morphology terminology used in this paper is adapted from Szalay and Delson (1979). Crown dimensions of the original specimens were measured to the nearest 0.1 mm with a sliding vernier caliper (Mitutoyo, Kanagawa Prefecture, Japan) by R.T. Kono. Crown mesiodistal (MD) length and buccolingual (BL) breadth were measured using the methods described in White (1977), Suwa (1990) and Suwa et al. (2009).. For all molars and fourth premolars, MD was measured along the MD axis of the crown that roughly bisects the tooth. BL is the maximum breadth measured along an axis perpendicular to the MD axis. In either case, the caliper jaws were applied to the specimen vertical to the occlusal plane. For the P_3s, we measured the longest diameter, maximum oblique diameter at crown base (MAXOB), instead of MD and the maximum diameter perpendicular to MAXOB, PP, instead of BL. For the P^3s, MD was not measured at the bisecting axis, but at the maximum width, maximus mesiodistal length, which usually corresponds to the position of preparacrista (see Zhang, Jin, et al. 2014; Zhang, Kono, et al. 2014).

Microfocus computed tomography (micro-CT) of the *Gigantopithecus blacki* mandible and upper premolars was

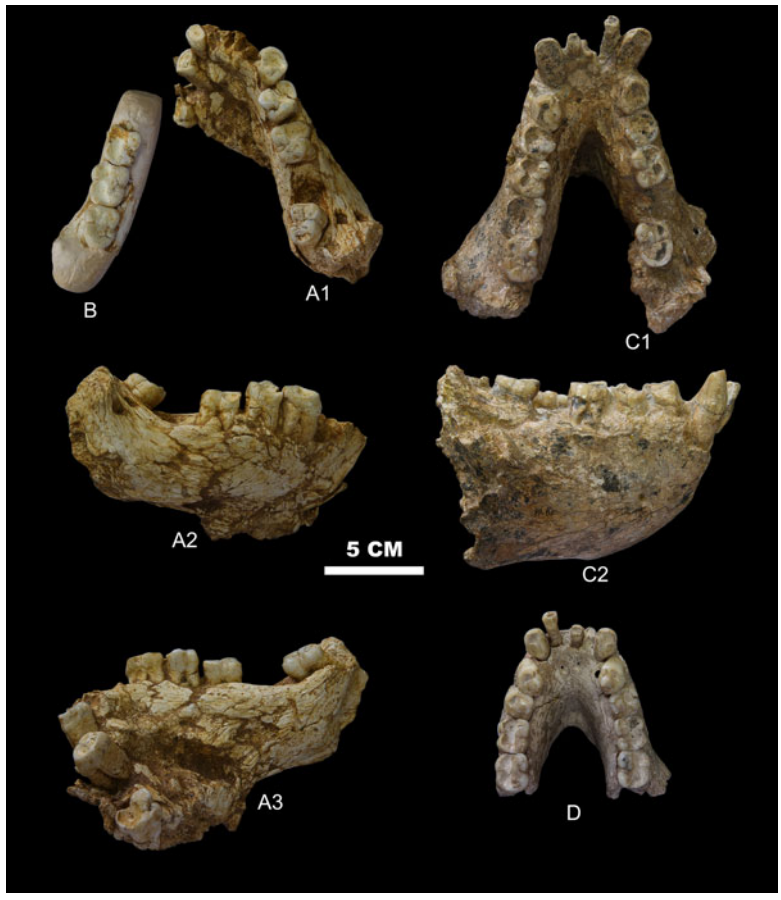

Figure 1. Mandibular remains of *Gigantopithecus blacki* from Yanliang Cave in comparison to Mandible III from the *Gigantopithecus* Cave, Liucheng, Guangxi. A, PA1601-1, a partial mandible with right P_3–M_1, M_3 and right C_1–P_4; B, PA1601-2 (occlusal view), a partial left corpus with M_{1-3} belonging to the same individual as PA1601-1; C, Mandible III (PA83); D, Mandible I (PA77). 1, Occlusal view; 2, right lateral view; 3, left medial view.

carried out using the 225-kV micro-CT system (developed by IHEP) at the KLVEHO. The specimens were scanned with beam energy of 140 kV and a flux of 100 mA at a detector resolution of around 40–120 μm per pixel using a 360° rotation with a step size of 0.5° and an unfiltered aluminum reflection target. A total of 720 transmission images were reconstructed in a 1024 × 1024 matrix of at most 781 slices using a two-dimensional reconstruction software developed by IHEP.

Systematic palaeontology

Order Primates Linnaeus, 1758

Superfamily Hominoidea Gray, 1825

Family Hominidae Gray, 1825

Subfamily Ponginae Elliot, 1913

Genus *Gigantopithecus* von Koenigswald, 1935

Species *Gigantopithecus blacki* von Koenigswald, 1935

(Figures 1 and 2)

For a list of newly referred material, see Table 1.

Description

Mandibular material

The material consists of two mandibular fragments that belong to a single individual, PA1601-1 (Figure 1(A)) and PA1601-2 (Figure 1(B)). PA1601-1 is a partially complete right corpus with P_3–M_1 and M_3, a crushed symphyseal region, and anterior part of the left corpus with C–P_4. The highly crushed symphysis and the anterior part of the left corpus are cemented together by matrix. The symphysis is badly deformed, but the alveoli for right I_1–C are arranged approximately in their original anatomical positions. The upper part of the right corpus below M_1–M_3, is best preserved. The right corpus is undistorted, but heavily weathered with irregular cracks. Unfortunately, the lower margin of the corpus is not preserved, so it is not possible to measure its height. Posteriorly, it is preserved approximately to the junction of the corpus and ramus,

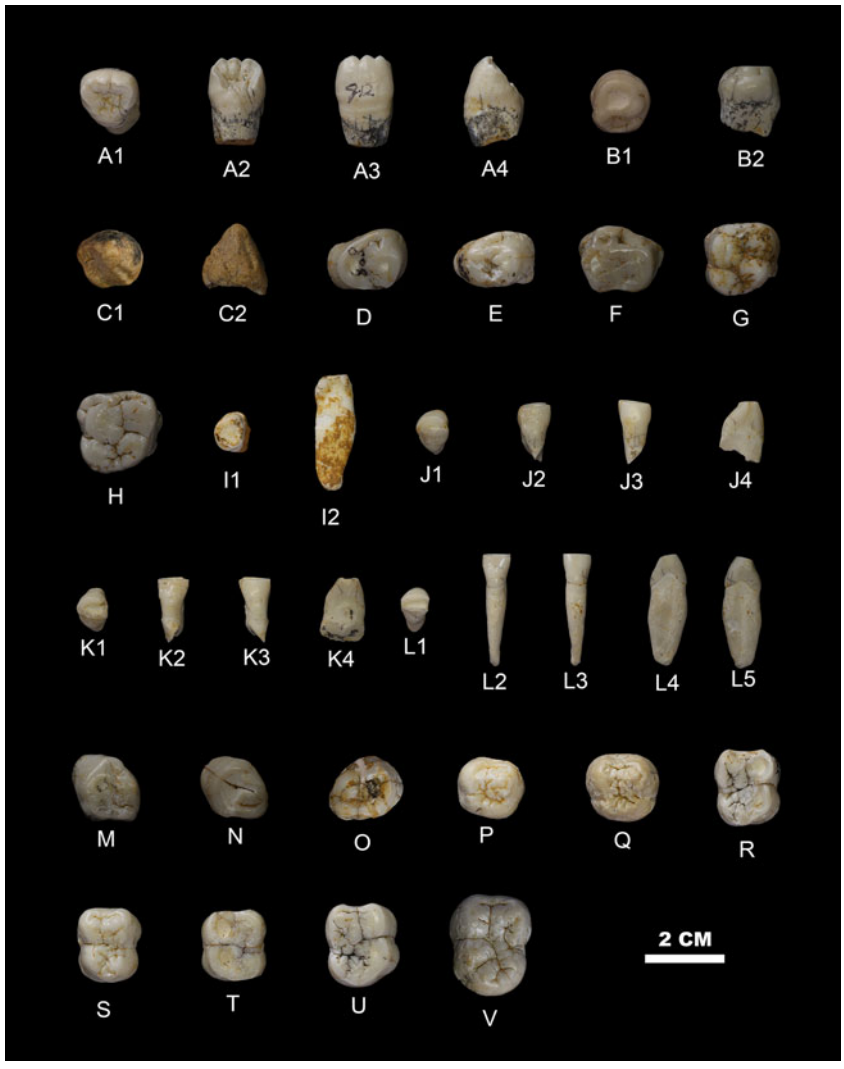

Figure 2. Dental remains of *Gigantopithecus blacki* from Yanliang Cave. A, PA1602.1, left I^1; B, PA1602.2, right C^1; C, PA1602.3, right C^1; D, PA1602.4, left P^3; E, PA1602.5, left P^3; F, PA1602.6, right P^3; G, PA1602.7, left $M^{1/2}$; H, PA1602.8, left M^3; I, PA1602.9, left I_1; J, PA1602.10, left I_2; K, PA1602.11, left I_1; L, PA1602.12, left I_1; M, PA1602.13, left P_3; N, PA1602.14, left P_3; O, PA1602.15, right P_3; P, PA1602.16, left P_4; Q, PA1602.17, left P_4; R, PA1602.18, right M_1; S, PA1602.19, left M_1; T, PA1602.20, left M_1; U, PA1602.21, right M_2; V, PA1602.22, left M_3. 1, Occlusal view; 2, lingual view; 3, buccal view; 4, mesial view; 5, distal view; occlusal view for the others.

similar to the condition in the Liucheng Mandible III (Figure 1(C)). The right P_3 and P_4 and their alveolar region are slightly displaced anteriorly compared with the better-preserved posterior portion. The premolars are displaced from their alveoli and exhibit excessive exposure of the roots. The roots of the right M1 are also exposed buccally due to breakage of the alveolar bone. The corpus is robust, and the lateral eminence is strongly developed opposite M_2, which contributes to the development of a wide extramolar sulcus. A small aperture resembling a mental foramen is located inferior to the posterior root of P_3, but its position is much higher than in the Liucheng mandibles. Using serial CT scan data, we have been able to confirm that it is not a mental foramen. On the medial surface of the corpus, a well-developed triangular torus envelops the roots of M_3. A broad and deep concavity is present just posterior to this torus. The wall of this concavity is positioned close to the distal root apex of the posterior molar. PA1601-2 is the posterior part of the left corpus with M_{1-3}. Only the alveolar portion of the body below the molars is preserved. Due to its fragility, it was detached from PA1601-1 during excavation. Because no meaningful morphological features are preserved on the partial corpus, the specimen was consolidated by plaster and moulded into the shape of a mandibular corpus.

All the teeth are moderately to heavily worn. Most of them have large areas of dentine exposure on the buccal cusps, except for the right M_3, which has dentine, exposed

distally instead. The basal cross-sectional outline of the left canine is a buccolingually elongated oval shape. It is heavily worn, with a large flat wear facet oriented perpendicular to the longitudinal axis of the tooth. A ledge-like enamel fold is present distolingually at the distal shoulder. Based on the size and morphology of the canine, the mandible belongs to a female individual. M_2 is larger than M_1 and M_3. M_3 tapers distally giving it an overall smaller size than M_2. The alveolus of the missing right M_2 is half -closed anteriorly, and posteriorly there is a wide and shallow depression surrounded by pathological bone. The depression continues to the base of the buccal root of M_3, and the mesial face of the M_3 does not show any interstitial contact facet. These observations indicate that the right M_2 had been lost during the individual's lifetime.

Upper incisor

PA1602.1 (Figure2(A)) is an unworn left upper central incisor. The root has been broken off about 5 mm from the buccal cervical margin. Its crown is robust and squat, with a somewhat triangular outline and nearly equal MD and BL dimensions. The buccal face is slightly convex. There are three distinct mammelons on the broad incisal margin of the tooth, which gives the incisal margin a zigzagged appearance. On the lingual side, the apical half of the crown is concave. Two marginal ridges, originating from the mesial and distal angles, respectively, border the central lingual fovea. The cervical half of the crown bulges lingually, and basal tubercules are present where the two marginal ridges meet. The cervical margin extends substantially onto the root buccally and lingually.

Two additional specimens, PA1602.23 and PA1602.24, both more worn than PA1602.1, are identified as left upper central incisors. It can be estimated that about two-thirds of the crown have been lost through wear in both specimens, but they preserve relatively complete roots. Their roots are approximately 20 mm in length when measured from the buccal cervical line. In both specimens, remnants of interstitial contact facets can be observed on the mesial and distal margins, and these help to determine the side. The wear facets, sloping to the distal side, and the occlusal outlines support the side identification.

Upper canines

PA1602.2 (Figure 2(B)) is a moderately worn right upper canine that can be assumed to have belonged to a female individual. The root has been gnawed by porcupines. The occlusal wear facet, forming a rounded dentine pit about 5 mm in diameter, is almost perpendicular to the longitudinal axis of the tooth. The basal cross-sectional outline is nearly circular. The mesial groove is narrow and shallow. The distal shoulder is more developed than the mesial one. The lingual cingulum can be observed leading from the distal shoulder, and several irregular pillars originate from the cingulum and pass towards the crown apex. The enamel margin extends substantially along the root on the buccal side. The enamel is quite thick, with a maximum thickness of 2.4 mm on the buccal rim of the occlusal facet.

PA1602.3 (Figure 2(C)) is a right upper canine germ of a presumed female individual. A sharp ridge marks the distal side of the tooth, which runs towards the cervix and ends at a moderately developed distal shoulder. A lingual marginal ridge runs from the distal shoulder, gives rise to several irregular ridges towards the crown apex, and ends at a lingual tubercle. A well-developed mesial groove originates from the mesial shoulder, but it is less well-developed than its distal counterpart. The cross-sectional contour at the cervix is nearly circular but slightly mesiodistally elongated.

Upper premolars

PA1602.4 (Figure 2(D)) is a moderately worn left P^3 with dentine exposure on the protocone and paracone. It has an asymmetric triangular occlusal outline. There is not much morphological detail left on the occlusal surface. The paracone is more elevated than the protocone. The buccal moiety is longer than the lingual moiety because of the mesially projecting preparacrista. All the roots are missing.

PA1602.5 (Figure 2(E)) is a slightly worn left P^3 with a tiny dentine pit on the paracone. Only the robust lingual root, approximately 28 mm in length, is preserved in its entirety. The tooth was three rooted because two separate root canals can be observed on the fractured surface of the buccal root. A strong invagination in the middle of the buccal root surface suggests that the divergence between the two radicles occurred more apically. The protocone and paracone are connected by a mesially convex crest, which also separates a large central fovea distally from a well-developed mesial fovea. The preprotocrista meets the preparacrista at the buccomesial corner of the crown and forms an angular projection. The postprotocrista runs buccally to meet the postparacrista. These two crests delimit the distal margin of the central fovea, with the hypoprotocrista and hypoparacrista representing the mesial margin.

PA1602.6 (Figure 2(F)) is a moderately worn right P^3 with dentine exposures on the protocone and paracone. Almost all the roots are missing and the pulp chamber is filled with matrix. Enamel hypoplasia is evident on the buccal wall of the tooth. The large anterior fovea, divided by a small longitudinal ridge, is bordered distally by the hypoprotocrista and the hypoparacrista and mesially by

the preprotocrista and the preparacrista. The base of the lingual wall is heavily worn with dentine exposure.

Upper molars

PA1602.7 (Figure 2(G)) is a lightly worn left $M^{1/2}$ without dentine exposure. The crown is mesiodistally longer than broad. The roots are missing, and there is slight damage to the crown along the distal and mesial walls and at the paracone tip. In occlusal view, the outline of the crown is rhomboidal, with the buccal cusps more mesially placed than the lingual cusps. The protocone is the largest of the main cusps, with the other three being subequal in size. The crista obliqua is intersected by a weak groove running between the paracone and hypocone. A narrow transversely aligned mesial fovea is present, delimited by a mesial marginal ridge, the preparacrista and the two mesial cusps. The posthypocrista and the postmetacrista do not quite meet, leaving the distal fovea open distally.

PA1602.8 (Figure 2(H)) is a slightly worn left M^3 without dentine exposure. The roots are mostly missing, but the fractured surface indicates the presence of three roots. The crown tapers distally, but its MD and BL dimensions are similar. The protocone is the largest cusp, and the metacone is relatively small. A ledge-like Carabelli's cusp is present, encircling the mesiolingual corner of the protocone. The mesial marginal ridge, together with the protocone and the paracone, delimits a narrow mesial fovea. The postmetacrista acts as the distal border of the distal fovea. Pit -like hypoplastic features are present on the mesiobuccal and lingual faces.

PA1602.25 represents half of a moderately worn $M^{1/2}$ crown. It was difficult to determine whether this is the mesial half of a left molar or the distal half of right molar. We provisionally recognise it as the latter because the exposed dentine patch on the lingual cusp is more marginally situated, indicating that the remaining lingual cusp is a hypocone rather than a protocone. If this identification is correct, the specimen is most probably a first molar because the MD corner forms a very acute angle. Also, the BL breadth of this tooth would have been greater than in the other two upper molars.

Lower incisors

PA1602.12 (Figure 2(L)) is a heavily worn left I_1 with considerable dentine exposure. The root is fully preserved. The root surface is concave both mesially and distally, but is more strongly so on the distal side. The crown narrows basally from the apex in lingual view. The buccal face of the tooth is slightly convex. A modest mesial marginal ridge borders the lightly concave lingual face, but there is no basal tubercle. Enamel thickness, measured on the buccal rim of the occlusal wear facet, is 1.2 mm.

PA1602.9 (Figure 2(I)) is a heavily worn left I_2 with extensive dentine exposure. The crown is asymmetrical. The worn occlusal surface slopes down towards the mesial side, which is an atypical wear pattern. However, exactly the same pattern can be seen on the lateral incisors of the Liucheng Mandible III. A shallow fovea occupies the central part of the lingual face, and is bordered basally by a narrow cingulum. The root is long, robust and mesiodistally compressed. The distal face of the root is only faintly grooved. The mesial notch of the cervical enamel line is more pronounced than its distal counterpart.

PA1602.10 (Figure 2(J)) and PA1602.11 (Figure 2(K)) are moderately worn left I_2 and I_1, respectively. Both crowns exhibit dentine exposure. The two incisors are likely to belong to a single individual because of the close fit between the interstitial contact facets and the thick enamel exposed on the occlusal wear facet (2.0 and 1.7 mm, respectively, on the buccal rim of the facet). The roots of the teeth have been gnawed by porcupines. The distal portion of the incisal edge slopes basally. There is no cingulum; instead, a low median basal bulge and a distal fovea are present. Again, the mesial cervical notches are more pronounced than their distal counterparts.

Lower premolars

PA1602.13 (Figure 2(M)) is a moderately worn left P_3. It is bicuspid with the protoconid larger than the metaconid. The cusps are separated by a median longitudinal groove. In occlusal view, the crown is rhomboidal in shape. The occlusal surface of the crown is worn nearly flat. The protoconid has a dentine pit about 3 mm in diameter. The enamel thickness measured on the buccal rim of the wear facet is 2.7 mm, although it is probably somewhat exaggerated by the obliquity of the wear. The preprotocristid and the premetacristid meet mesially and delimit the mesial fovea. The postprotocristid extends lingually to the distolingual margin of the metaconid and forms the distal margin of the distal fovea. The mesiobuccal face of the crown bulges buccally and bears a smooth honing facet produced by occlusion with the upper canine. The lingual face of the crown is nearly vertical. The cervix on the mesiobuccal face extends far inferiorly onto the root. The two roots are only partially preserved due to porcupine gnawing. The mesial and distal roots are subequal in size.

PA1602.14 (Figure 2(N)), a left P_3 and PA1602.15 (Figure 2(O)), a right P_3 exhibit a similar morphology to PA1602.13 (Figure 2(M)), except that the honing facet is less distinct. Both specimens bear prominent hypoplasial grooves, especially on the buccal faces. The roots of PA1602.14 are almost completely preserved. The buccal root is compressed mesiodistally, while the lingual root is buccolingually compressed. The roots of PA1602.15 are

not preserved, and the crown is damaged mesially and distally.

PA1602.16 (Figure 2(P)) and PA1602.17 (Figure 2(Q)) are unworn left P_4s. The former is smaller than the latter. The occlusal outline is trapezoidal, with the mesial moiety broader than the distal moiety. The two main cusps are transversely aligned and separated by a narrow median fissure. The metaconid is more elevated than the protoconid. The mesial fovea is narrow and groove-like, and bordered by the preprotocristid, premetacristid and the two main cusps. The distal marginal ridge, which bears three or four small tubercles, is separated from the main cusps by a deep groove. The talonid basin occupies the distal one-third of the crown. It is deep and well defined, being much larger than the mesial fovea.

Lower molars

PA1602.20 (Figure 2(T)) and PA1602.18 (Figure 2(R)) are moderately worn left and right M_1s, respectively. They both have considerable dentine exposure on the buccal cusps. Enamel thickness measured at the buccal rim of the protoconid wear facet, is 2.4 and 2.1 mm, respectively. The following description is mainly based on the nearly unworn left M_1, PA1602.19 (Figure 2(S)). The roots of all three teeth are not well preserved. The crown is elongated mesiodistally with some degree of waisting between the mesial and distal cusps. The metaconid is the largest cusp. The protoconid is slightly smaller, followed by the hypoconid and entoconid, with the hypoconulid being the smallest cusp. The crown exhibits pronounced buccal flare. The metaconid is rectangular in occlusal outline. Both the preprotocristid and the premetacristid extend medially to meet each other. Along with the mesial cusps, these two crests delimit the narrow groove-like mesial fovea. A trenchant longitudinal groove separates the protoconid from the metaconid. A deep transverse groove passes between the protoconid and hypoconid, and extends two -thirds down the buccal face of the crown.

PA1602.21 (Figure 2(U)) is a moderately worn right M_2 with only a tiny dentine pit on the hypoconid. The roots have been mostly removed by gnawing. The crown is not as mesiodistally elongated as in M_1. The buccal wall exhibits strong flare. A longitudinal groove passes between protoconid and metaconid, and a transverse one passes between the protoconid and hypoconid. The two grooves meet at a right angle near the distal margin of the protoconid. The metaconid is the largest cusp, followed by the hypoconid, protoconid and hypoconulid. The entoconid is the smallest cusp. The thickness of the enamel on the buccal rim of the hypoconid wear facet is 2.8 mm, but the value may be overestimated due to the obliquity of the wear. This specimen possibly belongs to the same individual as PA1602.18 (Figure 2(R)), because the interstitial contact facets correspond well and the degree of wear is consistent.

PA1602.22 (Figure 2(V)) is an unworn left M_3 with the roots missing. The tooth is long relative to its breadth. The largest cusp is the metaconid. The main crest of the metaconid originates at the buccodistal corner and passes buccally then distally (like a 'deflecting wrinkle'), to join the entoconid. The protoconid is the next largest cusp, followed by the hypoconid. The hypoconulid is much smaller, and is buccally displaced. All three buccal cusps are separated from each other by deep fissures. The groove passing between the protoconid and hypoconid extends far down on the buccal wall. Two accessory cupsules are present between the entoconid and the hypoconulid. The distalmost cuspule, which is the largest of the two, probably corresponds to a sixth cusp. A groove passes mesiodistally to separate the buccal cusps from the lingual cusps. The mesial fovea is represented by a transverse fissure bordered by the preprotocristid, premetacristid and the mesial cusps.

Comparisons and discussion

Because the Yanliang mandible (Figure 1(A),(B)) is poorly preserved, not much can be determined about its morphological characteristics. However, comparisons with the Liucheng mandibles, especially Liucheng Mandible III with comparable anatomical features preserved to those of the Yanliang mandible, do allow for several interesting observations to be made. The best preserved part of the right corpus is morphologically similar to the left side of Liucheng Mandible III (Figure 1(C)). In superior view, they both share a strongly laterally flaring ramus root with a wide extramolar sulcus lateral to M_3. It might be more flared in the Liucheng mandible, but since the bone surface of the Yanliang specimen is eroded, we cannot be certain. Medially, it is not possible to discern anatomical details of the Yanliang specimen, such as the course of the mylohyoid line or the development of the transverse torus. The posterior part of the corpus is better preserved, and there is a well-developed toral structure at the level of M_3, and a distinctive concavity just posterior to it. Unfortunately, the corresponding part of the mandible is not well preserved in Liucheng Mandible III, so it is not possible to make a direct comparison. Nevertheless, the remaining bone surface of the latter specimen suggests that a similar structure was present.

The degree and pattern of wear seen on the premolars and molars of the Yanliang mandible is similar to that seen in Liucheng Mandible III. Only the right M_3 differs, probably because the M_3 of the Yanliang mandible is tilted. When compared with Liucheng Mandible I (from an older adult female, Figure 1(D)), the premolars are much more worn in the Yanliang mandible. The wear facet on

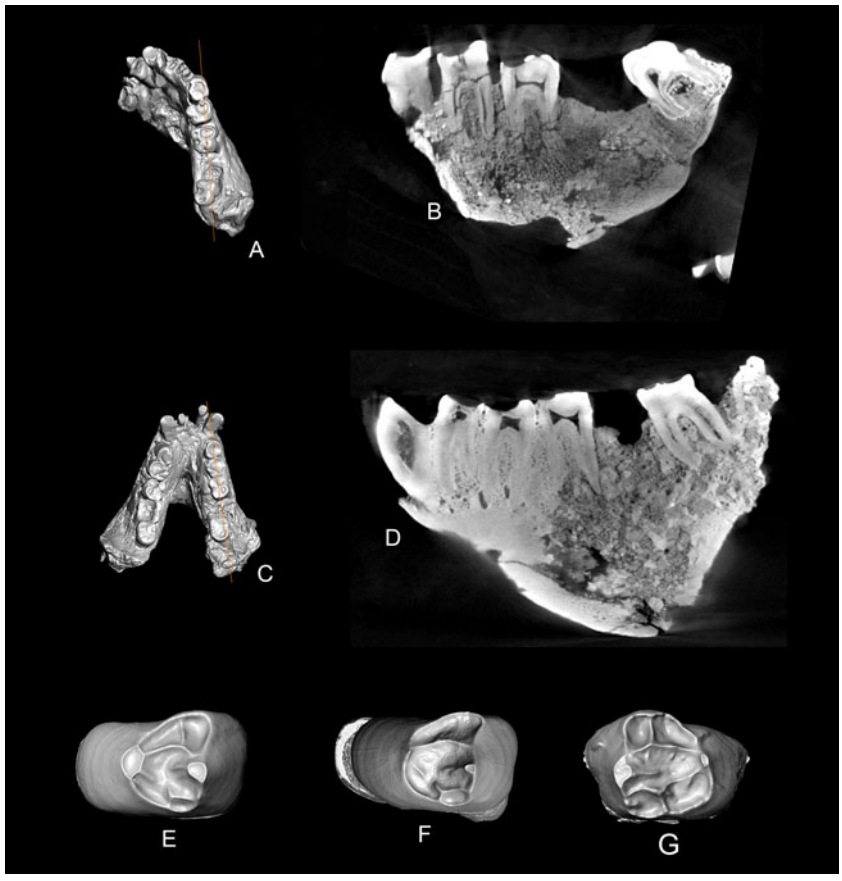

Figure 3. CT scanning sections for PA1601-1 and Liucheng Mandible III, and the EDJ morphology of PA1602.4, PA1602.5 and PA1602.6. A, CT section for PA1601-1; B, CT section for PA1601-1; C, CT section for Mandible III; D, CT section for the Mandible III; E, EDJ morphology of PA1602.4; F, EDJ morphology of PA1602.5; and G, EDJ morphology of PA1602.6.

the Yanliang canine is distinctive compared to the two Liucheng mandibles in being flat and almost perpendicular to the long axis of the tooth.

The Middle and Late Pleistocene hominins with severe antemortem tooth loss (AMTL) are often regarded as evidence of human-like behaviours, such as conspecific care or cooking (e.g. Lordkipanidze et al. 2005; Lebel et al. 2001). However, AMTL is not unique to hominins, but also occurs in non-human primates (Gilmore 2013). The occurrence of AMTL in fossil hominoids is seldom reported. The antemortem loss of the right M_2 in PA1601-1 is indicated by the partially resorbed socket. The vertical CT section of the Mandible III (Figure 3(C),(D)) shows the socket of the left M_2 is filled by matrix, while that of PA1601-1 (Figure 3(A),(B)) shows that the space between the right M_1 and M_3 is much wider than normal and that resorption has partially filled the alveolus of the lost right M_2 with bony tissue. There is an interstitial contact facet on the distal wall of the Yanliang right M_1, but the facet on the mesial wall of the right M_3 is not discernable. This indicates that the right M_2 was lost before eruption of the right M_3. The anteriorly tilted right M_3 also supports this assumption. The malocclusion was probably caused by the lack of resistance from the neighbouring M_2. Wear on the right M_3 confirms that even though it was tilted, it was still effective in chewing. However, the pattern of wear is not typical; only the hypoconulid was heavily worn with a large oval dentine exposure about 6 mm in diameter. The evidence suggests that the individual represented by PA1601-1 and PA1601-2 must have survived for a considerable period of time with impaired masticatory capabilities.

Zhang, Jin, et al. (2014) and Zhang, Kono, et al. (2014) analysed the upper premolar enamel–dentine junction (EDJ) complexity of *Gigantopithecus blacki* from Hejiang Cave, dated to 400–320 ka, as well as those from Early Pleistocene sites and drugstore collections. They concluded that the Hejiang Cave material represented a specialised form of *Gigantopithecus blacki* limited to the Middle Pleistocene and differing in premolar morphology complexity from those from the Early Pleistocene. The Middle Pleistocene Hejiang Cave upper premolars demonstrate a more complicated and crenulated outer enamel surface than those in the comparative Early

Pleistocene and drugstore samples due to the presence of secondary crests that radiate from the paracone and protocone and that originate from the preparacrista and postparacrista. The EDJ morphology of all three P^3s from Yanliang (Figure 3(E)–(G)) was compared with those analysed by Zhang, Jin, et al. (2014) and Zhang, Kono, et al. (2014). The overall EDJ morphology of all three P^3s falls in the variation range of *Gigantopithecus blacki* illustrated by Zhang, Jin, et al. (2014) and Zhang, Kono, et al. (2014). The major crests on the Yanliang P^3s are not as sharp as those from Hejiang Cave. Unlike the Hejiang P^3s, no minor crests are present on the Yanliang premolars, including those that radiate from the paracone. The postparacrista and the postprotocone crista on the Yanliang P^3s extend medially and join the distal margin of the occlusal fovea. The preprotocone crista joins the parastylar crest on all of the P^3s from Yanliang Cave. The wide sulcus that interrupts the mesial margin of the occlusal fovea is not present on any the P^3s from Yanliang Cave. The EDJ morphology of the P^3s from Yanliang Cave resembles that of *Gigantopithecus blacki* from Early Pleistocene cave sites, and it can be distinguished from the more specialised morphology seen in the P^3s from Hejiang Cave. This evidence is consistent with the Early Pleistocene age designation of the Yanliang Cave (Yan et al. 2014; Zhu et al. 2014).

Acknowledgements

We thank Yemao Hou for arranging the CT scanning; Yihong Liu, Yuan Wang, Min Zhu and Yaling Yan for their hard work in the field; and Wenshu Sun for preparation of the fossil material. We extend our gratitude to Gareth Dyke, Eric Delson and one anonymous reviewer for their helpful comments on an earlier version of the manuscript.

Disclosure statement

No potential conflict of interest was reported by the authors.

Funding

The research was supported by the Key Research Program of the Chinese Academy of Sciences (kzzd-ew-03), the National Science Fund for Talent Training in Basic Science [grant number J1210008], National Natural Science Foundation of China [grant numbers 41072013 and 41202017] and the Program of China Geological Survey [grant number 1212011220519].

References

Cameron DW. 2003. A functional and phylogenetic interpretation of the late Miocene Siwalik hominid *Indopithecus* and the Chinese Pleistocene hominid *Gigantopithecus*. Himalayan Geol. 24:19–28.

Chang Y, Wang L, Dong X, Chen WY. 1975. Discovery of a *Gigantopithecus* tooth from Bama District in Kwangsi. Vert Palasiatica. 13:148–154.

Chang Y, Wu M, Liu C. 1973. New discovery of *Gigantopithecus* teeth from Wuming, Kwangsi. Chin Sci Bull. 18:130–133.

Ciochon RL, Piperno DR, Thompson RG. 1990. Opal phytoliths found on the teeth of the extinct ape *Gigantopithecus blacki*: implications for paleodietary studies. Proc Nat Acad Sci USA. 87(20):8120–8124. doi:10.1073/pnas.87.20.8120.

Daegling DJ, Grine FE. 1994. Bamboo feeding, dental microwear, and diet of the Pleistocene ape *Gigantopithecus blacki*. South Afr J Sci. 90:527–532.

Eckhardt RB. 1975. *Gigantopithecus* as a hominid. In: Tuttle RL, editor. Paleoanthropology, morphology and palaeoecology. Mouton: The Hague; p. 105–127.

Gilmore CC. 2013. A comparison of antemortem tooth loss in human hunter-gatherers and non-human catarrhines: implications for the identification of behavioral evolution in the human fossil record. Am J Phys Anthropol. 151(2):252–264. doi:10.1002/ajpa.22275.

Han K, Zhao L. 2002. Dental caries of *Gigantopithecus blacki* from Hubei Province of China. Acta Anthropol Sin. 21:191–197.

Hsu C-H, Han K-X, Wang L-H. 1974. Discovery of *Gigantopithecus* teeth and associated fauna in Western Hopei. Vert Palasiatica. 12: 293–309.

Jin C, Qin D, Pan W, Tang Z, Liu J, Wang Y, Deng C, Zhang Y, Dong W, Tong H. 2009. A newly discovered *Gigantopithecus* fauna from Sanhe Cave, Chongzuo, Guangxi, South China. Chin Sci Bull. 54(5): 788–797. doi:10.1007/s11434-008-0531-y.

Kelley J. 2002. The hominoid radiation in Asia. In: Hartwig WC, editor. The primate fossil record. Cambridge: Cambridge University Press; p. 369–384.

Lebel S, Trinkaus E, Faure M, Fernandez P, Guérin C, Richter D, Mercier N, Valladas H, Wagner GA. 2001. Comparative morphology and paleobiology of Middle Pleistocene human remains from the Bau de L'Aubesier, Vaucluse, France. Proc Nat Acad Sci USA. 98(20): 11097–11102. doi:10.1073/pnas.181353998.

Lordkipanidze D, Vekua A, Ferring R, Rightmire GP, Agusti J, Kiladze G, Mouskhelishvili A, Nioradze M, de León MSP, Tappen M, Zollikofer CPE. 2005. Anthropology: the earliest toothless hominin skull. Nature. 434(7034):717–718. doi:10.1038/434717b.

Pei W. 1957. Discovery of *Gigantopithecus* mandible and other material in Liu-cheng district of central Kwangsi in South China. Vert Palasiatica. 1:65–72.

Pei W, Li Y. 1958. Discovery of a third mandible of *Gigantopithecus* in Liu-Cheng, Kwangsi, South China. Vert Palasiatica. 2:193–200.

Pei WC, Woo JK. 1956. New materials of *Gigantopithecus* teeth from South China. Acta Palaeontol Sin. 4:477–490.

Suwa G. 1990. A comparative analysis of hominid dental remains from the Shungura and Usno Formations, Omo Valley, Ethiopia [PhD thesis]. Berkeley, CA: University of California.

Suwa G, Kono RT, Simpson SW, Asfaw B, Lovejoy CO, White TD. 2009. Paleobiological implications of the *Ardipithecus ramidus* dentition. Science. 326(5949):69, 94–99. doi:10.1126/science.1175824.

Szalay FS, Delson E. 1979. Evolutionary history of the primates. New York, NY: Academic Press.

Takai M, Zhang Y, Kono RT, Jin C. 2014. Changes in the composition of the Pleistocene primate fauna in southern China. Quat Int. 354: 75–85. doi:10.1016/j.quaint.2014.02.021.

von Koenigswald GHR. 1935. Eine fossile Säugetierfauna mit *Simia* aus Südchina [A fossil mammalian fauna including Simia form South China]. Proceedings of the Koninklijke Nederlandse Akademie van Wetenschappen. SerB Palaeontol Geol Phys Chem Anthropol. 38: 872–879.

von Koenigswald GHR. 1952. *Gigantopithecus blacki* von Koenigswald, a giant fossil hominoid from the Pleistocene of Southern China. Anthropol Pap Am Mus Nat Hist. 43:292–325.

von Koenigswald GHR. 1958. *Gigantopithecus* and *Australopithecus*. Leech. 28:101–105.

Wang W. 2009. New discoveries of *Gigantopithecus blacki* teeth from Chuifeng Cave in the Bubing Basin, Guangxi, South China. J Hum Evol. 57(3):229–240. doi:10.1016/j.jhevol.2009.05.004.

Wang W, Potts R, Hou Y, Cheng Y, Wu H, Yuan B, Huang W. 2005. Early Pleistocene hominid teeth recovered in Mohui Cave in Bubing Basin, Guangxi, South China. Chin Sci Bull. 50(23):2777–2782. doi:10.1360/982004-614.

Weidenreich F. 1945. Giant early man from Java and South China. Anthropol Pap Am Mus Nat Hist. 40:1–134.

White TD. 1975. Geomorphology to paleoecology: *Gigantopithecus* reappraised. J Hum Evol. 4(3):219–233. doi:10.1016/0047-2484(75)90009-3.

White TD. 1977. New fossil hominids from Laetolil, Tanzania. Am J Phys Anthropol. 46(2):197–229. doi:10.1002/ajpa.1330460203.

Woo J-K. 1962. The mandibles and dentition of *Gigantopithecus*. Paleontol Sin New Ser D. 11:1–94.

Yan Y, Wang Y, Jin C, Mead JI. 2014. New remains of *Rhinoceros* (Rhinocerotidae, Perissodactyla, Mammalia) associated with *Gigantopithecus blacki* from the Early Pleistocene Yanliang Cave, Fusui, South China. Quat Int. 354:110–121. doi:10.1016/j.quaint.2014.01.004.

Zhang Y. 1982. Variability and evolutionary trends in tooth size of *Gigantopithecus blacki*. Am J Phys Anthropol. 59(1):21–32. doi:10.1002/ajpa.1330590104.

Zhang Y, Jin C, Cai Y, Kono R, Wang W, Wang Y, Zhu M, Yan Y. 2014. New 400–320 ka *Gigantopithecus blacki* remains from Hejiang Cave, Chongzuo City, Guangxi, South China. Quat Int. 354:35–45. doi:10.1016/j.quaint.2013.12.008.

Zhang Y, Kono RT, Jin C, Wang W, Harrison T. 2014. Possible change in dental morphology in *Gigantopithecus blacki* just prior to its extinction: evidence from the upper premolar enamel–dentine junction. J Hum Evol. 75:166–171. doi:10.1016/j.jhevol.2014.06.010.

Zhao LX, Zhang LZ. 2013. New fossil evidence and diet analysis of *Gigantopithecus blacki* and its distribution and extinction in South China. Quat Int. 286:69–74. doi:10.1016/j.quaint.2011.12.016.

Zhu M, Schubert BW, Liu J, Wallace SC. 2014. A new record of the saber-toothed cat *Megantereon* (Felidae, Machairodontinae) from an Early Pleistocene *Gigantopithecus* fauna, Yanliang Cave, Fusui, Guangxi, South China. Quat Int. 354:100–109. doi:10.1016/j.quaint.2014.06.052.